RICE UNIVERSITY

Terahertz Conductivity Assessment of Doped and Aligned Carbon Nanotubes

by

Cody Sewell

A Thesis Submitted
in Partial Fulfillment of the
Requirements for the Degree

Master of Electrical and Computer Engineering

Approved, Thesis Committee:

Junichiro Kono
Professor of Electrical and Computer Engineering, Physics and Astronomy, and Materials Science and NanoEngineering

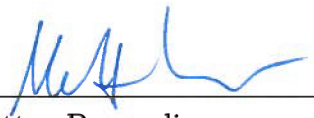

Matteo Pasquali
Chemical and Biomolecular Engineering, Chemistry, and Materials Science and NanoEngineering

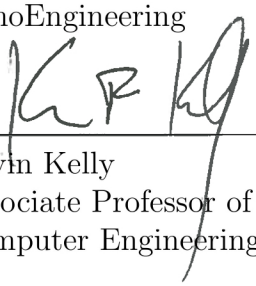

Kevin Kelly
Associate Professor of Electrical and Computer Engineering

Houston, Texas

April, 2017

ABSTRACT

Terahertz Conductivity Assessment of Doped and Aligned Carbon Nanotubes

by

Cody Sewell

Carbon nanotubes (CNTs) have captured the interest of scientists due to their usually large aspect ratios, as well as their remarkable optical, electrical and mechanical properties. A recent breakthrough has produced highly aligned nanotube films. Although these films are tightly packed, mono-domain and wafer-scale, their conductivity is lower than that of the theoretical maximum of single-wall CNTs or CNT fibers produced by wet spinning. Conductivity can be enhanced in these films via doping. Doping increases conductivity by decreasing the inter-tube resistance and increasing intra-tube conductivity. In this study, we investigated the potency and stability of six different dopants using terahertz time-domain spectroscopy. The results show that common high-redox potential acid dopants, such as nitric acid, are potent but volatile in stability. Dopants such as $AuCl_3$ (gold chloride) and F4-CNTQ are more effective and stable when used with CNT films.

Acknowlegments

My eternal cheerleaders, my family: you have always thought the most of me. You have always been enthusiastic in what I am doing and encouraging me to accomplish my best. Although some of you are no longer with me, you will be forever missed.

My friends and roommates, Jesse and Henry, thank you for the hobbies you sparked my interested in. Homebrewing and DIY-tinkering have been a great avenue of self-exploration and stress relief.

My oldest friend, Haibei, thank you for all the happy times. I am a better person for knowing you.

I am grateful to my lab colleagues who have provided invaluable support. Weilu Gao and Timothy Noe, I fear I will never be able to pay you back. Please know I would have not been able to complete this work without you.

A very special gratitude goes to my advisor, Jun Kono. Thank you for your patience and guidance. You have taught me the importance of scientific rigor in experimentation and reproducibility of data when developing conclusions. It is a philosophy that I feel transcends the lab and it will always be with me.

Contents

Illustrations

Chapter 1

Introduction

1.1 Carbon Nanotube Fundamentals

Carbon nanotubes (CNTs) garner much attention from both fundamental and applied researchers. It is thought of as an archetype of one-dimensional (1-D) systems. Essentially, CNTs are a rolled sheet of sp^2-bonded carbon atoms arranged in a honeycomb lattice– graphene. The manner in which a CNT is rolled introduce significant changes to its properties. Chirality vectors quantitatively describe the manner of rolling. These vectors are defined by the integer pair (n,m). When $n - m = 3v$ (v also an integer), the CNT is metallic; otherwise, it is semiconducting with a direct band gap. The band gap is inversely proportional to the diameter of the nanotube [2]. The variable chirality and closed 1-D topology, make for a system with a breadth of novel properties. Figure 1.1 illustrates the rolling of a carbon nanotube.

The 1-D topology of single-wall CNTs (SWCNTs) restricts carrier motion along the length of the tube. This results in electron mobilities of up to 10^5 cm^2V^{-1} at room temperature in individual nanotubes [3]. Semiconducting nanotubes posses great potential as the channel material in field-effect transistors (FETs). When fabricated from individual tubes, FETs have mobilities of 10^3 to 10^5 cm^2 $V^{-1}s^{-1}$ [4]. The 1-D topology of the CNT also produces van Hove singularities in the density of states, which result in strong optical absorption and emission [5].

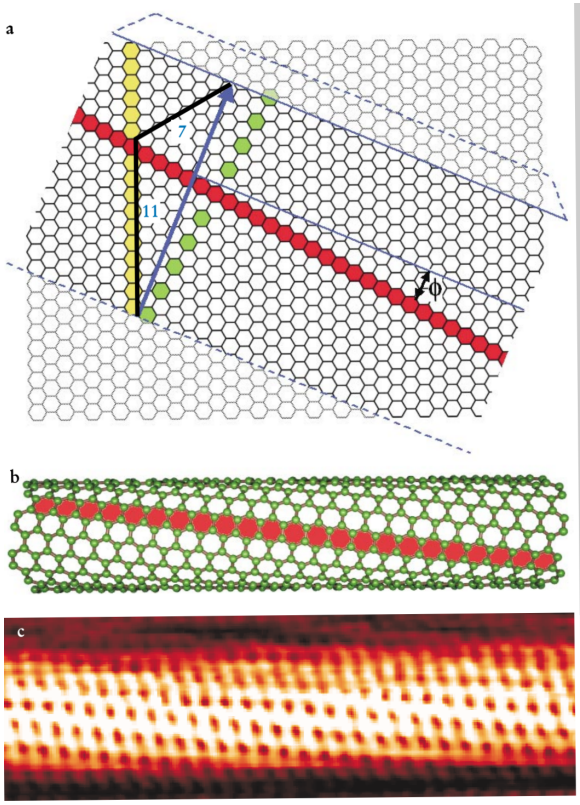

Figure 1.1 : Wrapping a CNT from a graphene lattice using transparent paper. Cut the transparent sheet with printed honey-comb lattice along the dashed lines indicated in **(a)**. Fold the sheet along the crease the causes the blue arrows tail to touch its head. Align the hexagons from the overlap tab with those on the tube body. Fasten the tube with tape. An (11,7) nanotube has now been rolled. This illustrates how the indices describe the projection of the circumferential vector (the blue arrow) onto the basis vectors of the graphene lattice. The red row illustrates the winding of the hexagons in the direction of the tube. The angle Φ is formed with respect to the tube axis. Wrapping the sheet along the yellow or green hexagonal rows form indices (n, m) zig-zag tubes or (n, n) armchair tubes with the hexagon rows parallel to the tube axis. **(b)** The resulting atomic structure of the tube made from above. **(c)** Atomically resolved scanning tunneling microscope (STM) image of a CNT [1].

Carbon nanotubes have potential applications in nano-scale electronics [6] and biological sensing [7]. Individual semiconducting SWCNTs have been used to produce field-effect transistors [8]. In order to scale up to devices, a macro-sized material is needed. This is accomplished by producing three-dimensional architectures of SWCNTs, including films, sheets, fibers, and ropes. Films avoid the challenge of material placement that is required for devices made from individual tubes. Also, the electronic properties of individual tubes are averaged out within a film. This leads to producing devices with more uniformity in electronic properties [4]. Thin-film transistors (TFTs) have been demonstrated from SWCNT films [9]. SWCNT films exhibit ultrabroadband light absorption that extends from ultraviolet to the terahertz (THz) regime, which make them an excellent candidate in optooelectronics. Semiconducting SWCNT (s-SWCNT) thin films can be layered with conjugate polymers to realize an infrared photodetector [10].

1.2 Previous Work and Motivation

Carbon nanotubes have great potential as an alternative to conventional conductor materials, such as copper and aluminum, and conventional semiconductor materials, such as silicon and gallium arsenide. Both of these applications benefit from having high conductivity. For metals, this would result in more efficient wires. For semiconductors, this would result in field-effect transistors with higher switching speeds. In fact, under the right conditions, when there is no scattering from defects or phonon modes, ballistic transport has been observed in individual SWCNTs [11] . Currently, the highest conductivity value for a bulk CNT material at room temperature is much lower at 5×10^6 S m^{-1} [12].

Several methods have been used to improve the electrical conductivity of CNT wires and films. CNT alignment and length are all reported to affect the conductivity of CNT networks [13][14]. As carriers in isotropically organized (unaligned) CNT films traverse more inter-CNT junctions per unit length, the scattering time decreases, which in turn decreases the conductivity. As anisotropy is introduced (i.e., tubes become aligned), there will be high conductivity along the direction of the tubes axis and lower conductivity perpendicular to the tube axis [15]. Although there have been recent breakthroughs in producing highly aligned CNT films, they still suffer short CNTs that comprise them [16].

Conductivity in CNT films can also be manipulated with doping. Studies have shown that acid treatment results in doping [17][18]. In the case of nanotube films, conductivity typically increases by four times [19]. Conductivity and transparency in SWCNT films are controlled by the interplay of localized and delocalized carriers. One study used doping along with tuning the ratio of metallic and semiconducting CNTs in a film in order to optimize transparency and conductivity [20]. In films, it was found that redox dopants increase the delocalized carrier density and the probability of electron transmission through intertube junctions. It was also found this was more effectively for semiconductor-enriched films than for metal-enriched films. [20]. As a result, we can conclude that doped semiconducting tubes have higher conductivity than intrinsic metal tubes. Doping has also been used to better understand how inter-tube and intra-tube carrier movement affect the overall conductivity of isotropic films. Conductive atomic force microscopy measurements identified two mechanisms in which nitric acid treatment affects isotropic nanotube networks [21]. One is increasing the the intrinsic conductivity of individual acid treated nanotubes. The other is

the reduction in junction resistance between individual tubes. The former increased conductivity $\sigma_{\text{intrinsic}} = (4.4 \pm 1.6)$ to $\sigma_{\text{doped}} = (5.6 \pm 1.2)$– a 30% increase. The latter decreased junction resistance by 3-fold [21]. From this, it is clear that decreasing junction resistance is the dominant mechanism in increasing film conductivity.

One of the most impressively high conductivity values in bulk CNT materials comes from wet spun CNT fibers. These fibers are dense, highly ordered and are comprised of long (5 μm) tubes. They are fabricated by dissolving tubes in chlorosulfonic acid. This solution is extruded through a spinneret to form a fiber. They have a conductivity of $2.9 \pm 0.3 \times 10^6$ S m^{-1} at room temperature. When doped with iodine the conductivity goes up to $5 \pm 0.5 \times 10^6$ S m^{-1} [12].

Recently, a breakthrough was made in producing highly-aligned, tightly-packed, monodomain, wafer-scale films of SWCNTs. These films have a conductivity of 2.5 $\times 10^5$ S m^{-1} [16], which is much lower than the previously mentioned wet-spun CNT fibers. These films provide a 2-fold opportunity in increasing conductivity: high physical alignment, which they already have, and manipulating Fermi level and intra-tube resistance via doping. In this study, we performed a comprehensive investigation one the potency and stability of a variety of dopants on highly-aligned, tightly-packed, monodomain, wafer-scale films of SWCNTs. We used six dopants: nitric acid (HNO_3), sulfuric acid (H_2SO_4), F4-TCNQ ($C_{12}F_4N_4$), gold chloride (Au_2Cl_6), iodine, and bromine. Dopants were chosen from different chemical families and states of matter in order to see their unique effect and time-dependent stability in manipulating the conduction of the SWCNT films. Nitric acid and sulfuric acid are strong acids and liquids. Gold chloride is a gold halide and was dissolved in water. Bromine is a halogen and was used in a near pure concentration. Iodine is a halogen and was

used to dope while vaporized. F4-TCNQ was dissolved in chloroform. It was chosen because it is one of the most widely used and most effective p-type dopants for many materials due to its strong electron-accepting ability.

Chapter 2

Experimental Methods

2.1 Sample Transfer

Large (>cm^2) monodomain highly aligned ($\pm 1.5^o$) films of SWCNTs produced by the arc-discharge method were used in all measurements. They were fabricated using slow vacuum filtration; a more detailed fabrication description can be found in previous work [16]. Due to the vacuum filtration process, the films come on a filter membrane. In order to transfer to arbitrary substrate, a wet transfer process was used to dissolve the filter membrane of the nanotube film onto an intrinsic Si (iSi) substrate. The procedure is as follows: 1) One or two drops of nanopure water were used to wet the iSi substrate. 2) The membrane/SWCNT film was placed onto the substrate with the nanotubes touching the surface. The film and substrate was mostly dried with compressed air and then allowed to completely dry in air for 5 minutes. This prevented the compressed air blowing away the film. 3) The substrate was bathed in heated (65°C) organic solvent N-methyl-2-pyrrolidone (NMP) for 20 minutes. 4) The substrate was then rinsed in acetone and then isopropyl alcohol and then dried in air. At this point, the CNT film was affixed to the iSi substrate with the filter membrane removed. The CNT film was examined with an optical microscope in order to check the orientation of the films and the uniformity of thickness.

2.2 Doping Mechanism and Process

In order to dope the samples, six dopants were used: nitric acid (HNO_3), sulfuric acid (H_2SO_4), F_4-TCNQ ($C_{12}F_4N_4$), gold chloride (Au_2Cl_6), iodine, and bromine. All of the dopants are p-type, and are effective due to strong electron-accepting abilities. The mechanism is also shared between these dopants. Firstly, these dopants do not introduce defects as substitutionary doping (common for traditional semiconductors) does. The CNT conductivity is enhanced via a charge transfer interfacial (between the wall of the tube and the dopant) doping mechanism. Electrons are donated (n-type) or withdrawn (p-type) without covalent modification to the wall. Therefore, the crystal and electronic structure of the CNT remains intact while the fermi level is raised or lowered via charge transfer.

Nitric acid stock was used at a molarity of 15M. Sulfuric acid stock came with a molarity 17M. It was diluted to 15M with chloroform (has less volatile reaction than water) such that the strong acid dopants would have matching molarities. 30.330 mg of gold chloride was weighted out using a scale accurate to ± 1 μg. This was disolved in 20 mL of water to yield a molarity of 5 mM. 2.21 mg of F4-TCNQ was weighed out using the same scale. This was dissolved in 20 mL of chloroform resulting in a molarity of 0.4 mM. Bromine was used in its pure form. All liquid dopants were poured into a petri dish until the liquid depth could cover the height of the sample. The sample was placed in the bath with Teflon coated tweezers (to prevent any reaction between the strong acid and tweezers). The sample left in the bath for 2 hours, removed, and then dried with nitrogen gas. Three, 10 g chunks of iodine were placed in an oven with the sample. The oven was heated to 200°C which would vaporize the iodine. The sample was left in the oven for 24 hours.

2.3 Experimental Apparatus

In order to investigate the effects of doping on CNT films, THz spectroscopy was used to measure transmittance, which can be converted to conductivity. Transmittance is the fraction of transmitted power, P, to the incident power P_{i}. It is calculated from the division of two measurements– reference and sample. Both are measurements of the transmitted intensity of the THz waveform in the time domain. These time-domain measurements are Fourier Transformed to the frequency domain to yield the power as a function of frequency. These two power spectra are divided, which yield transmittance. As a function of frequency, it is express as;

$$T(\omega) = \frac{P(\omega)}{P_{\mathrm{i}}(\omega)} \tag{2.1}$$

These measurements were performed with a commercial THz time-doman spectroscopy system (Advantest Model TAS7500). This provided the THz emitter and detector. The THz beam from the emitter is divergent and had to be collimated were then focused in order for it to be shone onto the sample. Collimating and focusing optics were placed in between the emitter and detector in order to achieve this. In this setup, all mirrors were parabolic. The optical setup is illustrated in Figure 2.1. Due to limited space on the optical table, all of the optics needed to be contained on a 9in by 9in breadboard. This allowed the optics to be removed when measurements were not being performed and replaced with minimal alignment work.

In order to measure the transmittance of only the aligned CNT films, sources of THz absorption must be eliminated. One of the most intrusive sources of THz absorption is from water vapor. Rotational transition changes in water cause many absorption lines in spectra [22][23]. Water vapor can be removed by creating a sealed area containing

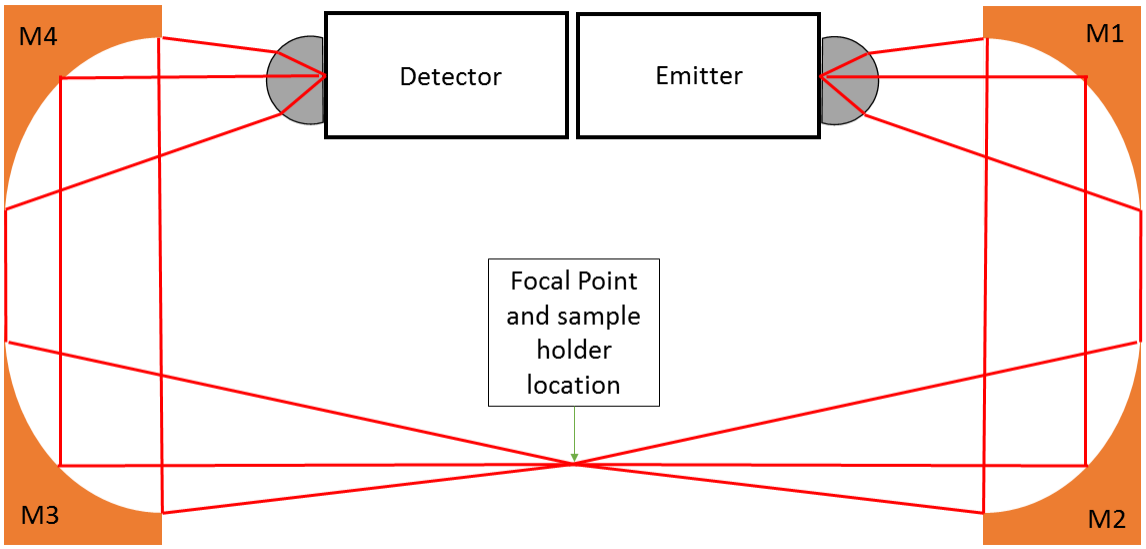

Figure 2.1 : Mirror M1 collimates the light from the emitter. It is a 1in focal length 1in diameter mirror. It is placed 1in from a virtual point source that is 2cm behind the hemispherical lens. The collimated light is then focused onto the sample with mirror M2– a 4in focal length and 2in diameter parabolic mirror. After passing through the sample, the light is then collimated with mirror M3– a 4in focal length and 2in diameter parabolic mirror. Lastly mirror M4, a 1in focal length 1in diameter parabolic mirror, focuses the light into the detector

the THz optical path. Although more permanent purge boxes are constructed from Plexiglass, our setup needed to be temporary and quickly reproducible. This was also because the optical setup needed to be easily moved and replaced. The solution was to use plastic wastebasket liner. The liner can slip over the breadboard loaded with optics and the edges can be tapped to the optical table. Eighth inch tubing was ran from the combination of a Porter-Cable air compressor and Advantest dry air unit to underneath the liner in order to purge the area. The relative humidity (RH) was

monitored with a humidity sensor. Thirty minutes of purging was required to achieve a relative humidity of less than 10%. One hour of purging was required to achieve a fluctuation in RH of less than 1%.

Before purging, the sample was loaded onto a sample holder inside the purge area. The sample holder consist of a Newport RSP-1T 360^{o} rotational stage. Inside its 1in bore a 1in aluminum plug was screwed in. The aluminum plug has a 4 mm aperture in the center. The sample was secured atop the aperture using a small amount of double-sided carbon tape. The rotational stage allows the sample's tubes angle with respect to the polarization of the THz wavefront. The stage was rotated until the THz waveform was most attenuated. This corresponds to the CNT films being parallel to the THz waveform. At this point, the THz waveform was measured in the time domain. Averaging was used to increase the signal-to-noise (S/N) ratio. In order to achieve an S/N of approximately 1/1000, 4096 measurements were taken and averaged together. This was done automatically in the Advantest software. This measurement took approximately 15 minutes. Afterwards, the sample was removed by slightly opening the plastic lining. The reference (bare iSi) was loaded and the purge was allowed to recover to the original RH level (usually about 10 minutes).

The resulting time-domain THz waveforms were used to calculate transmittance as described above.

Chapter 3

Results

3.1 Results

There are two values calculated for each sample's measurements: the parallel orientation transmittance, and the conductance. Both are functions of frequency. They are defined below where $T(\omega)$ is parallel transmittance, $P_{\mathrm{CNT}}(\omega)$ is the transmitted power spectrum of the CNT sample, $P_{\mathrm{ref}}(\omega)$ is the transmitted power spectrum of the intrinsic silicon.

$$T_{\mathrm{CNT}}(\omega) = \frac{P_{\mathrm{CNT}}(\omega)}{P_{\mathrm{ref}}(\omega)} \tag{3.1}$$

In order to calculate the conductance, the thin film conductance equation is used. It is defined below where σ is the conductance, $\alpha = \frac{1}{137}$, $z_{\mathrm{o}} = 377\Omega$, and n is the index of refraction of intrinsic silicon.

$$T_{\mathrm{CNT}}(\omega) = \left(1 + \frac{\alpha\pi}{1+n} z_{\mathrm{o}}\sigma\right)^{-2} \tag{3.2}$$

Equation 3.2 was solved for conductance. Figures 3.1 - 3.6 plot conductance as function of frequency, ω, for each dopant. All figures contain multiple traces for measurements taken over the period of hours to days.

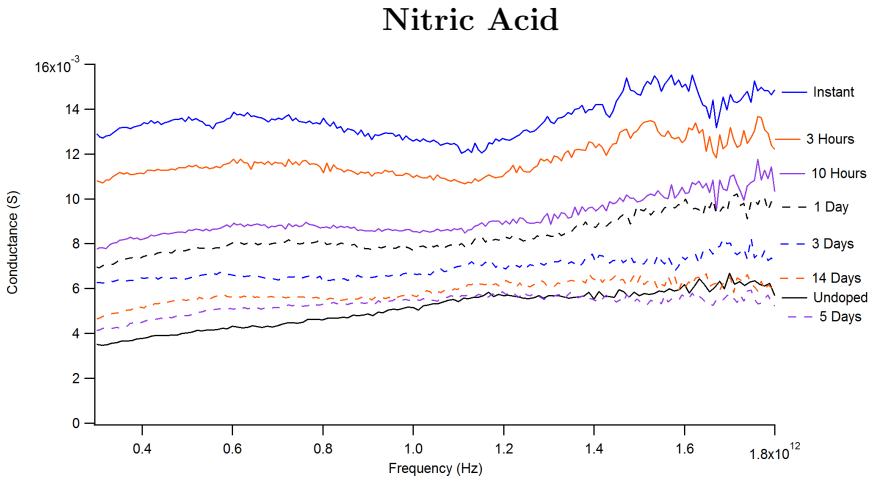

Figure 3.1 : Conductance of CNT film doped in 15M nitric acid solution for 2 hours. Traces are measurements taken in time taken in increasing time intervals

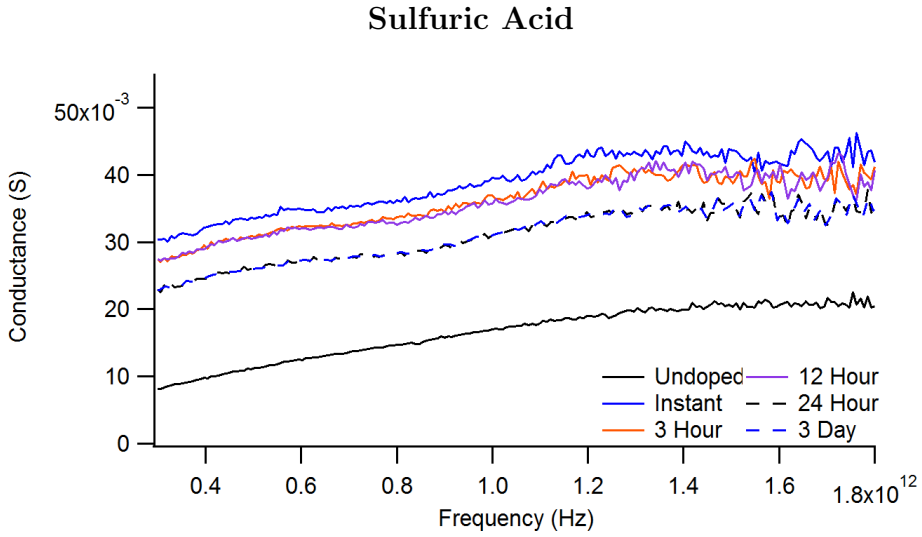

Figure 3.2 : Conductance of CNT film doped in 15M sulfuric acid solution for 2 hours. Traces are measurements taken in time taken in increasing time intervals

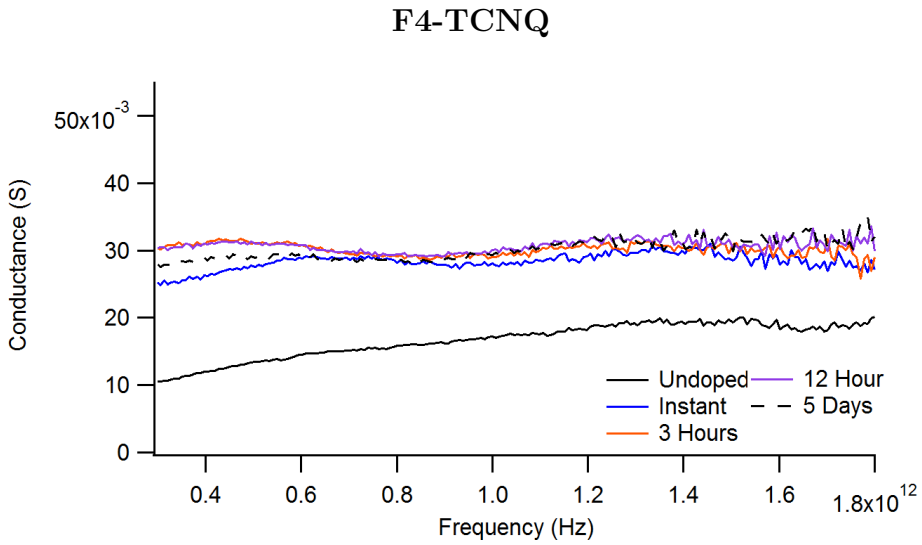

Figure 3.3 : Conductance of CNT film doped in 0.4mM F4-TCNQ solution for 2 hours. Traces are measurements taken in time taken in increasing time intervals

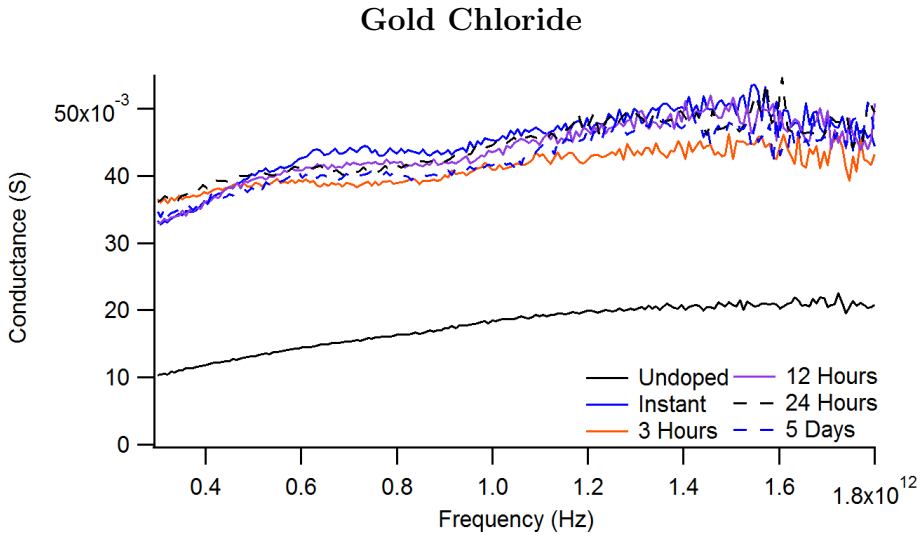

Figure 3.4 : Conductance of CNT film doped in 5mM gold chloride solution bath for 2 hours. Traces are measurements taken in time taken in increasing time intervals

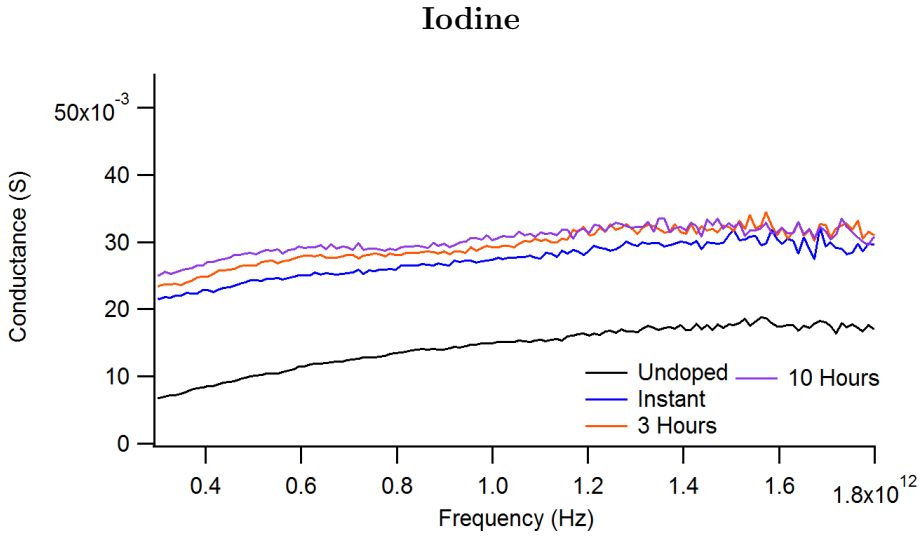

Figure 3.5 : Conductance of CNT film doped in vaporized iodine for 24 hours. Traces are measurements taken in time taken in increasing time intervals

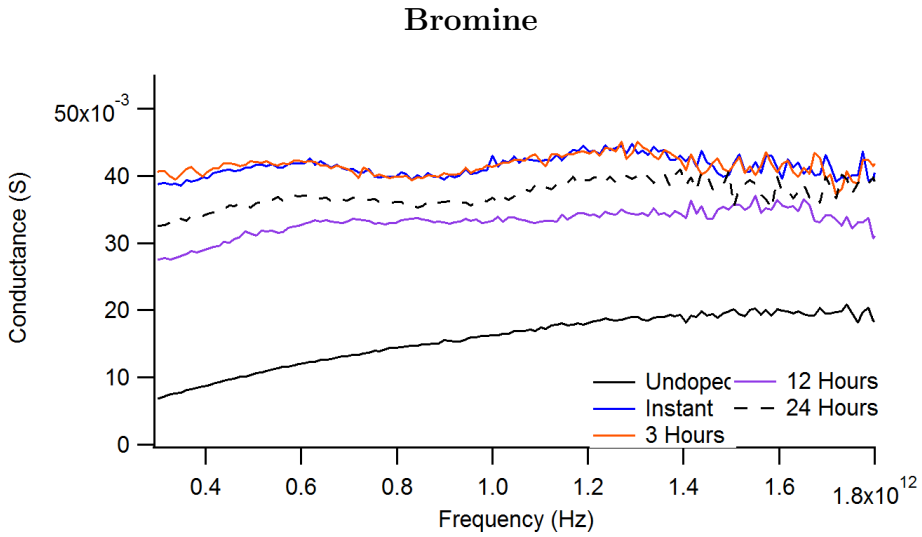

Figure 3.6 : Conductance of CNT film doped in pure bromine for 2 hours. Traces are measurements taken in time taken in increasing time intervals

In order to quantify the change in conductance, the percent difference in conductance is calculated just after doping and after doing has stabilized. This is done by calculating the average conductance before doping, just after doping, and after doping has stabilized. The averages are taken from the range of 0.3 THz to 1.8 THz. Equations 3.3 and 3.4 define the percent difference in conductance just after doping and percent difference in conductance after doping has stabilized, respectively, where σ_{u} is average conductance before doping, σ_{i} is average conductance just after doping, and σ_{f} is average conductance after doping has stabilized.

$$\frac{\sigma_{\mathrm{i}} - \sigma_{\mathrm{u}}}{\sigma_{\mathrm{u}}} \times 100\% \tag{3.3}$$

$$\frac{\sigma_{\mathrm{f}} - \sigma_{\mathrm{u}}}{\sigma_{\mathrm{u}}} \times 100\% \tag{3.4}$$

Figure 3.7 summarizes these results. Each dopant has a pair of bars that correspond to the percent difference in conductance just after doping and percent difference in conductance after doping has stabilized.

Percent Difference in Conductance just after doping and after doping has stabilized

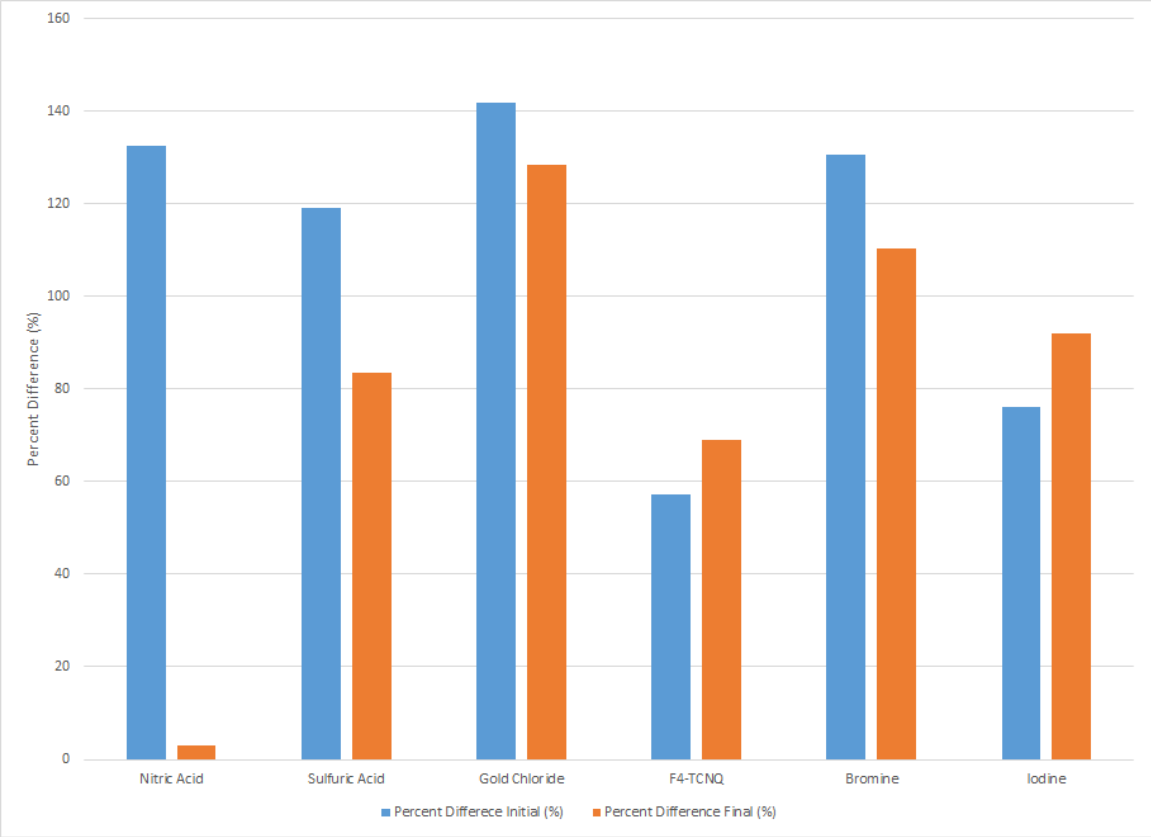

Figure 3.7 : Each dopant has a pair of bars that corresponds to the percent difference in conductance just after doping and percent difference in conductance after doping has stabilized. The blue bar corresponds to the percent difference in conductance just after doping. The orange bar corresponds to the percent difference in conductance after doping has stabilized. Dopants from left to right are nitric acid (HNO_3), sulfuric acid (H_2SO_4), gold chloride (Au_2Cl_6), F_4-TCNQ ($C_{12}F_4N_4$), bromine, and iodine

Chapter 4

Discussion

4.1 Nitric Acid

The first dopant tested was nitric acid. It is a good benchmark for stability as its doping effect gradually dissipates. The decay of the conductance is clearly seen in Figure 3.1. The curve labeled 'undoped' is the conductance measurement of the CNT film before doping. The next curve labeled 'instant' is the measurement taken instantly after the CNT film has been bathed in nitric acid for 2 hours. Between these two measurements, the percent change in average conductance is 135%. Already we can see the strong effect that doping has on the films. The next measurements are taken in increasingly longer time spans. This allows us to see the stability of dopant over time. After 14 days, the conductance is only 2% higher than the undoped value. Nitric acid has the 2^{nd} most percent increase in conductance just after doping, but almost returns to the undoped conductivity after 14 days. This makes it the least stable of the dopants.

4.2 Sulfuric Acid

Sulfuric acid, like nitric acid, is a strong acid dopant. The dopant is more stable over time than nitric. As can be seen in Figure 3.2, the last two measurements after doping, 24 hours and 3 days, almost perfectly overlap. It is not until after 12 hours does the conductance recede toward the original undoped measurement curve. After

3 days, the average conductance is 84% higher than before doping. Sulfuric acid is the 4^{th} highest percent change in conductance after doping and is the 5^{th} most stable.

4.3 F4-TCNQ

Unlike the previously discussed dopants, F4-TCNQ it is not an acid and is a solid at room temperature. In Figure 3.3 we see the behavior of a stable dopant. All curves following the undoped measurement overlap each other within just a few percent. It is the least change in percent difference of conductance out of all the dopants; however, it is the most stable because the conductance just after doping and after doping has stabilized have the least difference.

4.4 Gold Chloride

Gold Chloride, another non-acid dopant, has a similarly stability to F4-TNCQ. Gold Chloride has the greatest percent difference increase in conductivity– 142%. It is the 2^{nd} most stable dopant over time.

4.5 Bromine

Bromine has the 3^{rd} most increase in percent difference in conductivity just after doping. Its conductance begins to recede to the original conductance after 3 hours. It is the 4^{th} most stable dopant.

4.6 Iodine

Unlike the other measurements, this was not a bath based doping process. Instead, several chunks of iodine were vaporized in an oven with the sample also inside the

oven. It was immersed in the vapor for 24 hours before measuring its effect. It has 5^{th} most increase in conductance percent difference and is the 3^{rd} stable dopant.

Chapter 5

Conclusion

Our motivation in this work was to close the performance gap of conductivity between our carbon nanotube films and other highly conductive carbon nanotube based materials. Doping can assist in this by increasing the Fermi level and decreasing tube-tube junction resistance. Dopants that are effective in initially increasing conductivity may not be stable over long periods of time. At first, a strong dopant, nitric acid lost almost all of its effect over the course of two weeks. Finding a dopant that is effective over long periods of time is just as important. Gold chloride and F4-TCNQ were the most stable dopants.

There are a couple of future prospects to further investigate conductivity on aligned carbon nanotubes. One would be to use n-type dopants such as polythyleneimine [24], benzyl viologen [25], and phosphine derivatives [26]. The long term stability of these dopants have not been investigated on the films used in this study. All of the dopants used in this study were p-type. Another technique to increase the absorption would be to stack the CNT films or even sandwich dopants between CNT film layers [27]. This would have the advantage of not only increasing absorption but also sealing in dopants. Such endeavors make aligned CNT films an exciting material for next-generation devices.

Bibliography

[1] C. Dekker, "Carbon Nanotubes as Molecular Quantum Wires," *Physics Today*, May 1999.

[2] S. Reich, C. Thomsen, and J. Maultzsch, "Wiley: Carbon Nanotubes: Basic Concepts and Physical Properties - Stephanie Reich, Christian Thomsen, Janina Maultzsch."

[3] T. Drkop, S. A. Getty, E. Cobas, and M. S. Fuhrer, "Extraordinary Mobility in Semiconducting Carbon Nanotubes," *Nano Lett.*, vol. 4, pp. 35–39, Jan. 2004.

[4] S. Park, M. Vosguerichian, and Z. Bao, "A review of fabrication and applications of carbon nanotube film-based flexible electronics," vol. 5, pp. 1727–1752, Feb. 2013.

[5] S. M. Bachilo, M. S. Strano, C. Kittrell, R. H. Hauge, R. E. Smalley, and R. B. Weisman, "Structure-Assigned Optical Spectra of Single-Walled Carbon Nanotubes," *Science*, vol. 298, pp. 2361–2366, Dec. 2002.

[6] T. Pichler, M. Knupfer, M. S. Golden, J. Fink, A. Rinzler, and R. E. Smalley, "Localized and Delocalized Electronic States in Single-Wall Carbon Nanotubes," *Phys. Rev. Lett.*, vol. 80, pp. 4729–4732, May 1998.

[7] F. Valentini, S. Orlanducci, M. L. Terranova, A. Amine, and G. Palleschi, "Carbon nanotubes as electrode materials for the assembling of new electrochemical

biosensors," *Sensors and Actuators B: Chemical*, vol. 100, pp. 117–125, June 2004.

[8] P. Avouris, Z. Chen, and V. Perebeinos, "Carbon-based electronics," *Nat Nanotechnol*, vol. 2, pp. 605–615, Oct. 2007.

[9] C. Wang, J.-C. Chien, K. Takei, T. Takahashi, J. Nah, A. M. Niknejad, and A. Javey, "Extremely Bendable, High-Performance Integrated Circuits Using Semiconducting Carbon Nanotube Networks for Digital, Analog, and Radio-Frequency Applications," *Nano Lett.*, vol. 12, pp. 1527–1533, Mar. 2012.

[10] M. S. Arnold, J. D. Zimmerman, C. K. Renshaw, X. Xu, R. R. Lunt, C. M. Austin, and S. R. Forrest, "Broad Spectral Response Using Carbon Nanotube/Organic Semiconductor/C60 Photodetectors," *Nano Lett.*, vol. 9, pp. 3354–3358, Sept. 2009.

[11] J. Kong, E. Yenilmez, T. Tombler, W. Kim, H. Dai, R. Laughlin, L. Liu, C. Jayanthi, and S. Wu, "Quantum interference and ballistic transmission in nanotube electron waveguides," *Physical Review Letters*, vol. 87, 2001.

[12] N. Behabtu, C. C. Young, D. E. Tsentalovich, O. Kleinerman, X. Wang, A. W. K. Ma, E. A. Bengio, R. F. t. Waarbeek, J. J. d. Jong, R. E. Hoogerwerf, S. B. Fairchild, J. B. Ferguson, B. Maruyama, J. Kono, Y. Talmon, Y. Cohen, M. J. Otto, and M. Pasquali, "Strong, Light, Multifunctional Fibers of Carbon Nanotubes with Ultrahigh Conductivity," *Science*, vol. 339, pp. 182–186, Jan. 2013.

[13] H. Dai, "Carbon nanotubes: opportunities and challenges," *Surface Science*, vol. 500, pp. 218–241, Mar. 2002.

[14] J. D. Harris, R. P. Raffaelle, T. Gennett, B. J. Landi, and A. F. Hepp, "Growth of multi-walled carbon nanotubes by injection CVD using cyclopentadienyliron dicarbonyl dimer and cyclooctatetraene iron tricarbonyl," *Materials Science and Engineering: B*, vol. 116, pp. 369–374, Feb. 2005.

[15] W. A. deHeer, W. S. Bacsa, A. Chtelain, T. Gerfin, R. Humphrey-Baker, L. Forro, and D. Ugarte, "Aligned Carbon Nanotube Films: Production and Optical and Electronic Properties," *Science*, vol. 268, pp. 845–847, May 1995.

[16] X. He, W. Gao, L. Xie, B. Li, Q. Zhang, S. Lei, J. M. Robinson, E. H. Hroz, S. K. Doorn, W. Wang, R. Vajtai, P. M. Ajayan, W. W. Adams, R. H. Hauge, and J. Kono, "Wafer-scale monodomain films of spontaneously aligned single-walled carbon nanotubes," *Nat Nano*, vol. 11, pp. 633–638, July 2016.

[17] R. Graupner, J. Abraham, A. Vencelov, T. Seyller, F. Hennrich, M. M. Kappes, A. Hirsch, and L. Ley, "Doping of single-walled carbon nanotube bundles by Brnsted acids," vol. 5, pp. 5472–5476, Jan. 2003.

[18] V. Skkalov, A. B. Kaiser, U. Dettlaff-Weglikowska, K. Hrnarikov, and S. Roth, "Effect of Chemical Treatment on Electrical Conductivity, Infrared Absorption, and Raman Spectra of Single-Walled Carbon Nanotubes," *J. Phys. Chem. B*, vol. 109, pp. 7174–7181, Apr. 2005.

[19] H.-Z. Geng, K. K. Kim, K. P. So, Y. S. Lee, Y. Chang, and Y. H. Lee, "Effect of Acid Treatment on Carbon Nanotube-Based Flexible Transparent Conducting Films," *J. Am. Chem. Soc.*, vol. 129, pp. 7758–7759, June 2007.

[20] J. L. Blackburn, T. M. Barnes, M. C. Beard, Y.-H. Kim, R. C. Tenent, T. J. McDonald, B. To, T. J. Coutts, and M. J. Heben, "Transparent Conductive Single-

Walled Carbon Nanotube Networks with Precisely Tunable Ratios of Semiconducting and Metallic Nanotubes," *ACS Nano*, vol. 2, pp. 1266–1274, June 2008.

[21] P. N. Nirmalraj, P. E. Lyons, S. De, J. N. Coleman, and J. J. Boland, "Electrical Connectivity in Single-Walled Carbon Nanotube Networks," *Nano Lett.*, vol. 9, pp. 3890–3895, Nov. 2009.

[22] R. T. Hall and J. M. Dowling, "Pure Rotational Spectrum of Water Vapor," *The Journal of Chemical Physics*, vol. 47, pp. 2454–2461, Oct. 1967.

[23] M. v. Exter, C. Fattinger, and D. Grischkowsky, "Terahertz time-domain spectroscopy of water vapor," *Opt. Lett., OL*, vol. 14, pp. 1128–1130, Oct. 1989.

[24] M. Shim, A. Javey, N. W. Shi Kam, and H. Dai, "Polymer Functionalization for Air-Stable n-Type Carbon Nanotube Field-Effect Transistors," *J. Am. Chem. Soc.*, vol. 123, pp. 11512–11513, Nov. 2001.

[25] S. M. Kim, J. H. Jang, K. K. Kim, H. K. Park, J. J. Bae, W. J. Yu, I. H. Lee, G. Kim, D. D. Loc, U. J. Kim, E.-H. Lee, H.-J. Shin, J.-Y. Choi, and Y. H. Lee, "Reduction-controlled viologen in bisolvent as an environmentally stable n-type dopant for carbon nanotubes," *J. Am. Chem. Soc.*, vol. 131, pp. 327–331, Jan. 2009.

[26] Y. Nonoguchi, K. Ohashi, R. Kanazawa, K. Ashiba, K. Hata, T. Nakagawa, C. Adachi, T. Tanase, and T. Kawai, "Systematic Conversion of Single Walled Carbon Nanotubes into n-type Thermoelectric Materials by Molecular Dopants," *Scientific Reports*, vol. 3, p. 3344, Nov. 2013.

[27] N. Komatsu, W. Gao, P. Chen, C. Guo, A. Babakhani, and J. Kono,

"Modulation-Doped Multiple Quantum Wells of Aligned Single-Wall Carbon Nanotubes," *Adv. Funct. Mater.*, vol. 27, pp. n/a–n/a, Mar. 2017.